Swimming behavior and prey retention of the polychaete larvae Polydora ciliata (Johnston)

Hansen, Benni Winding; Jacobsen, Hans Henrik; Andersen, Anders; Almeda, Rodrigo; Pedersen, Troels Møller; Christensen, Anette M.; Nilsson, Birgitte

Swimming behavior and prey retention of the polychaete larvae *Polydora ciliata* (Johnston)

B. W. Hansen[1], H. H. Jakobsen[2,*], A. Andersen[3], R. Almeda[4], T. M. Pedersen[1], A. M. Christensen[1] and B. Nilsson[1]

[1]Roskilde University, Department of Environmental, Social and Spatial Change, P O Box 260, DK-4000 Roskilde, Denmark, [2]National Institute of Aquatic Resources, Charlottenlund Slot, Jægersborg Allé 1, DK-2920 Charlottenlund, Denmark, [3]Department of Physics and Center for Fluid Dynamics, Technical University of Denmark, DK-2800 Kgs. Lyngby, Denmark and [4]Institut de Ciències del Mar, CSIC P. Marítim de la Barceloneta 37-49, 08003 Barcelona, Spain

*Author for correspondence at present address: National Environmental Research Institute, Aarhus University, Frederiksborgvej 399, P.O. Box 358, DK-4000 Roskilde, Denmark (hhja@dmu.dk)

SUMMARY

The behavior of the ubiquitous estuarine planktotrophic spionid polychaete larvae *Polydora ciliata* was studied. We describe ontogenetic changes in morphology, swimming speed and feeding rates and have developed a simple swimming model using low Reynolds number hydrodynamics. In the model we assumed that the ciliary swimming apparatus is primarily composed of the prototroch and secondarily by the telotroch. The model predicted swimming speeds and feeding rates that corresponded well with the measured speeds and rates. Applying empirical data to the model, we were able to explain the profound decrease in specific feeding rates and the observed increase in the difference between upward and downward swimming speeds with larval size. We estimated a critical larval length above which the buoyancy-corrected weight of the larva exceeds the propulsion force generated by the ciliary swimming apparatus and thus forces the larva to the bottom. This modeled critical larval length corresponded to approximately 1 mm, at which, according to the literature, competence for metamorphosis and no more length increase is observed. These findings may have general implications for all planktivorous polychaete larvae that feed without trailing threads. We observed bell shaped particle retention spectra with a minimum prey size of approximately 4 μm equivalent spherical diameter, and we found that an ontogenetic increase in maximum prey size add to a reduction in intra-specific food competition in the various larval stages. In a grazing experiment using natural seawater, ciliates were cleared approximately 50% more efficiently than similar sized dinoflagellates. The prey sizes retainable for *P. ciliata* larvae covers the microplankton fraction and includes non-motile as well as motile prey items, which is why the larvae are trophically positioned among the copepods and dinoflagellates. Not only do larval morphology and behavior govern larval feeding, prey behavior also influences the feeding efficiency of *Polydora ciliata*.

Key words: *Polydora ciliata*, low Reynolds number hydrodynamics, swimming behavior, prey selection.

INTRODUCTION

Spionid polychaetes are some of the most common benthic invertebrates of neritic environments. Hence, during certain periods, their planktotrophic larvae are very abundant in coastal waters. They reach concentrations >1000 l⁻¹ and are a major component of the zooplankton community (Anger et al., 1986; Zajac, 1991; Bochert and Brick, 1996; Pedersen et al., 2008). Spionids are one of the most common and widespread polychaete families in the Oslofjord, Norway (Schram, 1968) and in the Iseford complex, Denmark (Rasmussen, 1973) from which the present larval material was collected. Among spionids, *Polydora ciliata* is one of the dominant species, with a wide geographic distribution in Northwest Europe, and it is also found in Australian and Japanese waters as an introduced species (NIMPIS, 2002). *P. ciliata* larvae may be the single most dominant polychaete larvae in neritic waters and reach concentrations >500 l⁻¹ and their potential trophic role cannot be neglected (Daro and Polk, 1973, Pedersen et al., 2008; Pedersen et al., 2010).

Fig. 1 shows *P. ciliata* in the early, intermediate, and late larval stage. *Polydora* spp. larval morphology is described in detail by Wilson (Wilson, 1928), Hannertz (Hannertz, 1956), Blake (Blake, 1969) and Plate and Husemann (Plate and Husemann, 1994). Based on the detailed sketches by Wilson (Wilson, 1928), we presume that the ciliary swimming apparatus is primarily composed of a band of closely spaced cilia (the prototroch), surrounding approximately three-quarters of the head circumference, and secondarily by a band of cilia around the terminal segment (the telotroch). Many spionids lack feeding cilia ('metatroch') and food groove, and must therefore capture particles using alternative mechanisms (Pernet and McArthur, 2006). This is most likely the case for *P. ciliata* larvae.

Data on particle size retention in polychaete larvae are scarce. For example, the upper limit for ingestible particle size increased with larval size for *Streblospio benedicti* (Pernet and McArthur, 2006) and also for a gastropod veliger. For the gastropod veliger it was simply explained by changes in morphological dimensions of the feeding apparatus (velum structures) (Hansen, 1991). The linkage between particle retention mechanism and the morphology of the ciliary feeding apparatus are not reported for *Polydora* larvae. In the spionid *Marenzelleria* cf. *viridis* phytoplankton <20 μm were the principal dietary component and a maximum prey diameter of 80 μm is described for larvae with 6–10 segments (setigers) (Burckhart et al., 1997). *Polydora* has been reported to have been reared on microalgae (Anger et al., 1986), and Daro and Polk (Daro and Polk, 1973) reported small phytoplankters and even invertebrate larvae as prey. No comprehensive uptake efficiencies of a coherent broad regime of prey sizes are reported for any spionid larvae.

Here we address prey size selectivity and the swimming patterns of *Polydora* larvae following offerings of different sized prey either as single species or as mixtures of *in situ* prey. To facilitate the

Fig. 1. Differential interference contrast (DIC) microscope images of early, intermediate and late *Polydora ciliata* larvae. The images are composed of multiple layers from different focal planes sliced through the larvae and software-merged into the final images. The larvae were fixated with a few drops of saturated $MgCl_2$. Apart from some body contraction, the fixation did not seem to damage the larvae.

interpretation of the observed development in ontogenetic swimming behaviors we developed a simple swimming model based on low Reynolds number hydrodynamics. Using the modeling approach we further interpreted our observations of the maximum clearance rate and its dependence on larval size. Thus our aim was to explore the interaction between functional morphology and behavioral components in spionid larval suspension feeding.

MATERIALS AND METHODS
Larval collection
Live zooplankton was collected from surface water (0–2.5 m) with a 50 μm WP-2 net equipped with a non-filtering cod-end by horizontal trawling at slow speed. The sampling station 'Søminestationen' (55°44′N, 11°48′E) is situated in the Isefjord, Denmark, and it is shallow with muddy bottom sediments and eutrophic waters. Once the net was retrieved, zooplankton was gently transferred to an isothermic container, diluted with surface water, and transported to the laboratory within 2 h of collection. In the laboratory, *P. ciliata* larvae were concentrated using a cold fiber optic light source, sorted with a pipette under the dissecting microscope and placed in a beaker with 0.2 μm filtered seawater (FSW) from the sampling area. In order to reduce contamination by other planktonic organisms, the larvae were washed repeatedly by transferring them through a series of Petri dishes with 0.2 μm FSW until ambient phytoplankton were absent.

Swimming behavior
Swimming of *P. ciliata* larvae (*N*=58) of various lengths was studied in a $15{\times}15{\times}15\,cm^3$ acrylic aquarium at a temperature of 20°C and a salinity of 15 PSU. The setup allowed us to visualize swimming trajectories spatially and estimate true three-dimensional swimming velocities and behaviors. Briefly, a mirror was mounted transversely inside the aquarium allowing direct observations of larvae and their mirrored images simultaneously. Illumination was provided by an infrared light-emitting diode placed perpendicular to the camera. The diode was positioned in the focal point of a Fresnel lens (diameter 16 cm), thus creating parallel (collimated) light beams in the experimental aquarium and in turn mirrored into a monochrome analogue CCD video camera (Minitron MTV-1802CD, Minitron Enterprise Company, Taipei, Taiwan) fitted with a 105 mm lens. Size calibration was done by filming a ruler and converting pixels to millimeters. Video observations were recorded on a VHS tape recorder. After recording the video sequences of interest were digitized using a Pinnacle movie box™ (Pinnacle Systems, Mountain View, CA, USA) into QuickTime™. Movies and motion tracks were analyzed using a motion analysis software package (LabTrack, Bioras.dk, Nivå, Denmark). After the motion tracks were digitized, three-dimensional tracks were reconstructed by merging each motion track with the mirror track manually. Larval swimming was studied in three prey regimes: filtered seawater, filtered seawater with *Rhodomonas salina* added as small prey, and filtered seawater

Table 1. *Polydora ciliata* larval swimming speed in three different prey regimes

Prey species (size, ESD)	V_{down} (mm s^{-1} ± s.d.)	N	V_{up} (mm s^{-1} ± s.d.)	N	V (mm s^{-1} ± s.d.)	N
Filtered seawater	1.03±0.39	5	0.43±0.11	4	0.66±0.25	2
Rhodomonas salina (9 μm)	0.82±0.46	16	0.35±0.22	8	0.45±0.10	9
Akashiwo sanguinea (53 μm)	1.02±0.43	15	0.46±0.19	12	0.62±0.19	8

ESD, equivalent spherical diameter.

Table 2. Characteristics of the *Polydora ciliata* larval stages used in the feeding experiments

Larval stage	Length (μm)	Number of setigers	Biomass (μg C)**	Prototroch cilia length (μm)	Telotroch cilia length (μm)
Early	220±18	3.5±0.8	0.270	26.8±1	25±8
Intermediate	561±27	8.9±1.7	0.982	44.5±8	32.3±8.8
Late*	919±16	13.3±1.9	1.941	48.1±3	32.3±11

*With palps. **Larval carbon biomass was calculated based on length (Hansen, 1999).
Values are means ± s.d.

with *Akashiwo sanguinea* added as large prey (Table 1). Length and diameter of live animals (N=57) were estimated from size-calibrated video frames in the software package ImageJ (http://rsbweb.nih.gov/ij/index.html).

Cilia measurements

A sub-sample of (N=25) live larvae of a wide range of development sizes was sedated with a few drops of MgCl$_2$ in a small 4 mm deep micro-well and lengths of the prototroch, the telotroch and the larval body were measured. Larvae were separated in three groups according to size (Table 2). The MgCl$_2$ was applied until the larvae ceased moving. Apart from inducing body shrinkage, MgCl$_2$ seemed not to damage the larvae, as they recovered after a short period of time and resumed swimming. The larvae were photographed under a microscope at 100× magnification and the images were subsequently analyzed using the software package ImageJ.

Maximum clearance and ingestion rates

The functional response for three different development stages of *P. ciliata* larvae fed the diatom *Thalassiosira weissflogii* was determined. The full data-sets are presented elsewhere (Almeda et al., 2009). Larvae were separated into three groups according to size (Table 2). Subsamples of larvae from each size group (N=25–30) were fixed in 5% acid lugol solution, and the average lengths and numbers of setigers were determined using an inverted microscope. Initial grazing trials with aged tank seawater turned out unsuccessfully and instead 0.2 μm filtered seawater from the sampling area was used. *Thalassiosira weissflogii* were provided from a stock culture growing in B1 medium (Hansen, 1989). Stock phytoplankton concentrations and the size (equivalent spherical diameter; ESD) of *Thalassiosira weissflogii* were determined by a Multiziser III Coulter Counter electronic particle counter (Beckman Coulter, Miami, FL, USA). The cell carbon quota used was 131 pg C cell^{-1} (Dutz et al., 2008). Each grazing trial was executed in triplicate grazing bottles with parallel triplicate phytoplankton growth controls. Average concentrations of larvae ranged from 2.6 to 1.0 larva ml^{-1} for early and late larval stage, respectively. The phytoplankton suspensions were amended with a nutrient mixture to compensate for nutrient enrichment due to larvae excretion. The incubations were carried out in 70 ml blue cap glass bottles mounted with plastic film before closing to prevent inclusions

of air bubbles. Bottles were incubated for 24 h on a slowly rotating plankton wheel (0.5 r.p.m.) in a temperature-controlled room at 16°C and constant dim light (<5 μmol photons m^{-2} s^{-1}).

Cell concentrations in grazing and control trials were determined by a CytoBuoy scanning flow cytometer (CSFC; CytoBuoy b.v., Woerden, The Netherlands). The CSFC is designed to process live phytoplankton particles larger than 1 μm. In this study we counted around 0.5 ml samples in triplicate. The prey cell in the experimental trials was counted by leaving the CSFC sample suction tube directly into the incubation bottles. During counting, the trial bottles were carefully stirred with a mechanical stirrer set at the lowest r.p.m. Prior to starting a series of grazing trials, we compared the counting performance of CSFC to the electronic particle counter and found no significant deviation between the instruments (Almeda et al., 2009). Clearance and ingestion rates were calculated for each food concentration according to Frost (Frost, 1972) after the verification that prey growth rates in grazing bottles were significantly lower than in the prey growth controls (one-way ANOVA, P<0.05) and the maximum rates derived from the functional response equations.

Particle size selection

We conducted experiments to examine larval feeding efficiency as a function of particle size for early and late larval stages. The two stages were separated from collected larvae according to their size. Larvae were offered potential prey of different size (ESD) ranging from 4 to 53 μm (Table 3). Otherwise the experimental procedure was as described above. The experiments were performed with one phytoplankton species per experimental treatment and with an equal initial phytoplankton biomass (0.2 μg C ml^{-1} and 1 μg C ml^{-1} for early and late larval stages, respectively). The prey retention efficiencies

Table 3. Phytoplankton species used in the prey size selection experiment and their dimensions

Phytoplankton species	ESD (μm)	Cell volume (μm³)
Isochrysis galbana	4	34
Rhodomonas salina	9	357
Thalassiosira weissflogii	13	1124
Heterocapsa triquetra	19	3591
Akashiwo sanguinea	53	79,730

Particle sizes were estimated as outlined in Materials and methods.
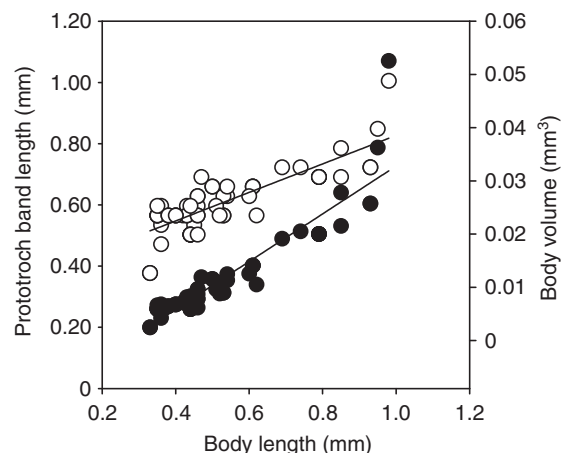ESD, equivalent spherical diameter.

Fig. 2. Morphometric relationships of *Polydora ciliata* larvae. Larval circumference (prototroch cilia band length) is plotted *versus* larval body length (white circles; left axis), and larval body volume is plotted *versus* larval body length (black circles; right axis).
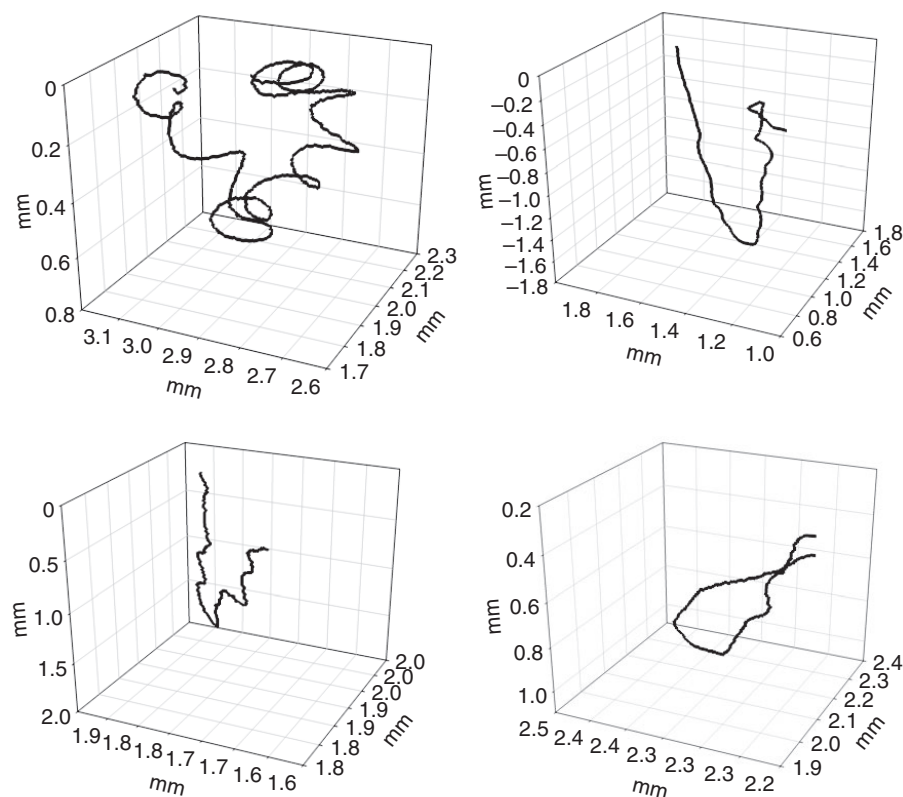
Fig. 3. Four examples of reconstructed three-dimensional swimming paths of *Polydora ciliata* larvae showing the typical helical structure of some paths and the large overall path variation.

are given as the clearance rates on the different sized prey, according to Frost (Frost, 1972).

Grazing on natural prey

The experiments consisted of incubations of natural microplanktonic communities with the addition of *P. ciliata* larvae for the experimental treatments. Natural seawater (NSW) for grazing incubations was collected at 1 m depth with a Niskin bottle and screened through a 200 μm mesh by reverse filtration in order to exclude mesozooplankton. The water was amended with a nutrient mixture to compensate for nutrient enrichment due to larval excretion. Twelve 70 ml blue cap bottles were filled with NSW. Then 75 late-stage larvae approximately 900 μm long, were added to six of the NSW-containing bottles. Two bottles with larvae and two without larvae were fixed with 1% acidic Lugol's solution to determine the initial microplankton abundance. The remaining eight bottles consisting of four grazing bottles and four control bottles were incubated for 24 h on a plankton wheel (0.5 r.p.m.) in a temperature-controlled room at 16°C and constant dim light.

Ciliate, dinoflagellate and diatom abundance was estimated by settling 10 ml aliquots in Utermöhl chambers for 24 h in two replicates per treatment and counted under an inverted microscope. Digital images of each cell type were taken and sized with the open source software package ImageJ. Cell volumes were converted into carbon content using a factor of $0.19\,\mathrm{pg\,C\,\mu m^{-3}}$ (Putt and Stoecker, 1989) whereas the carbon of dinoflagellates and diatoms were estimated accordingly to the recommendations of Menden-Deuer and Lessard (Menden-Deuer and Lessard, 2000). Grazing was calculated if prey types in grazing trails were significantly different from controls (one-way ANOVA, $P<0.05$). Clearance and ingestion rates were calculated for each prey type according to Frost (Frost, 1972).

RESULTS
Morphometrics of live larvae

The body length (*l*) of the larvae that we used for motion analysis ranged from 0.3 mm to 1.0 mm (Fig. 2). The diameter of the larval head and hence the circumference of the prototroch cilia band increased as the larval body length increased. The number of setigers increased from typically three to 13 during growth (Fig. 1 and Table 2). The diameter of the larvae (*d*) ranged from 0.16 mm to 0.26 mm and *l*/*d* increased by a factor of two during growth from *l*/*d*=1.9 on average for the early larval stage to *l*/*d*=3.8 on average for the late larval stage and hence the larvae did not grow isometrically (Fig. 2). The prototroch cilia were of comparable length in the intermediate and late larval stages and in these stages the cilia were significantly longer than the cilia in the early stage (one-way ANOVA, $P<0.001$; Table 2). The telotroch cilia, however, seemed not to increase in length significantly during larval ontogeny and remained statistically invariable during the larval development (one-way ANOVA, $P=0.356$).

Swimming patterns and speeds

The larvae were swimming in helical paths and showed large individual variations (Fig. 3). A typical swimming path is a sequence of downwards, upwards, and horizontal trajectories. We tested swimming speed of the general swimming groups, i.e. horizontal, downwards and upwards swimming against prey and filtered seawater and found no significant differences in the swimming speed when different prey was offered (one-way ANOVA, $P>0.05$; Table 1). Furthermore we did not see any differences in swimming pattern and the data sets were pooled into one data set consisting of swimming paths divided into three groups based on the overall swimming direction: horizontal, downwards and upwards swimming. The average of all our measured horizontal swimming speeds (*V*) is $0.50\pm0.21\,\mathrm{mm\,s^{-1}}$ and we observed that the average
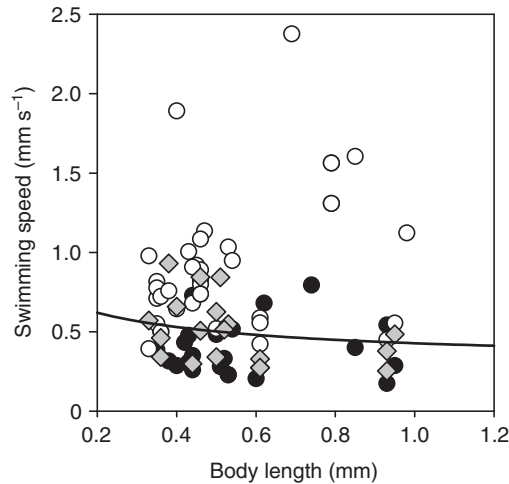
Fig. 4. Swimming speeds of *Polydora ciliata versus* larval body length. Measured swimming speeds: downward speed V_{down} (white circles); upward speed V_{up} (black circles); horizontal speed V (grey diamonds). The solid line indicates the theoretical model (Eqn 10) of the horizontal swimming speed.

horizontal swimming speed decreases slightly with increasing body length (Fig. 4). The larvae swam downwards significantly faster than they swam upwards: $V_{down}=0.93\pm0.40\,\mathrm{mm\,s^{-1}}$ *versus* $V_{up}=0.42\pm0.19\,\mathrm{mm\,s^{-1}}$ (*t*-test, *t*=5.6, d.f.=58, *P*<0.001) and the difference between the average upward and downward swimming speed increased with increasing body length. In the following we show that our observations on the swimming behavior can be explained using a simple swimming model based on low Reynolds number hydrodynamics and taking the effect of gravity on the slightly negatively buoyant larvae into account.

Swimming model

In our hydrodynamic model we assumed that each individual larva swims lengthwise with constant velocity due to the propulsion force generated by the ciliary swimming apparatus, and that the propulsion force is balanced by the drag on the larval body. We will not attempt to describe the helical swimming paths of the larvae, but only the observed average swimming speed. For simplicity we model the cigar shaped body of the larva as a prolate spheroid with polar radius a=body length/2 and equatorial radius b=body diameter/2.

From the measured body lengths (l) and horizontal swimming speeds (V) we can estimate the Reynolds number of the flow past the swimming larvae. We define the Reynolds number as:

$$Re = \frac{\rho l V}{\eta} , \qquad (1)$$

where ρ is the density of the water and η is the dynamic viscosity. For the larvae that swim horizontally we find that the Reynolds number ranges from Re=0.12 to Re=0.46. Since the typical Reynolds number is fairly low, it is a reasonable approximation to model the flow using Stokes' equation. The drag D on the larva is therefore proportional to both the larval size and the swimming speed:

$$D = C_D \eta a V , \qquad (2)$$

where C_D is a dimensionless drag coefficient that only depends on the geometrical shape of the larva. The drag D on a prolate spheroid with polar radius a and equatorial radius b, which is moving

lengthwise with constant speed at low Reynolds number is [see Happel and Brenner (Happel and Brenner, 1983), pp. 154-156]:

$$D = \frac{8 \pi \eta c V}{(\tau_0^2 + 1)\coth^{-1}\tau_0 - \tau_0} , \qquad (3)$$

where c is a geometrical parameter that is defined in the following way:

$$c = \sqrt{a^2 - b^2} , \qquad (4)$$

and where τ_0 is another geometrical parameter with the definition:

$$\tau_0 = a/c . \qquad (5)$$

Eqn 3 is exact and valid for all values of a/b, i.e. it is valid for both prolate spheroids with low a/b and slender prolate spheroids with high a/b. To explore the drag model for a/b in the range between 2 and 4, which is relevant for *P. ciliata* larvae, we would like to have a more simple analytical expression to work with than the exact Eqn 3. The often-used slender spheroid approximation [see Happel and Brenner (Happel and Brenner, 1983), p. 156; and Berg (Berg, 1993), pp. 55-58]:

$$D = \frac{4 \pi \eta a V}{\ln(2 a / b) - 1/2} , \qquad (6)$$

is not applicable in the present study, since it overestimates the drag considerably in the a/b range from 2 to 4 and is only a valid approximation of Eqn 3 when a/b is larger than 10. Instead we consider the following approximation [see White (White, 2006), pp. 171-172]:

$$D = \frac{6 \pi (4 + a / b) \eta b V}{5} . \qquad (7)$$

Eqn 7 gives a good approximation with less than 1% relative error in the a/b ratio range from 2 to 4 in comparison with the exact drag expression (Eqn 3), and since approximation (Eqn 7) is easy to work with and analyze we shall use it in the following. Inserting Eqn 7 into Eqn 2 and rearranging, we see that the drag coefficient becomes:

$$C_D = \frac{6 \pi (4 + a / b)}{5 a / b} , \qquad (8)$$

which decreases from C_D=(3/5) 6π with a/b=2 (early larval stage) to C_D=(2/5) 6π with a/b=4 (late larval stage). We note for comparison the well-known result that C_D=6π for a sphere.

The propulsion force F and the drag force D must have the same magnitude if the larva swims with constant velocity. We presume that the ciliary swimming apparatus consists primarily of the prototroch and secondarily of the telotroch cilia band. We do not have detailed observations of the metachronal wave motion in the cilia bands, and we therefore make some simplifying assumptions about the propulsion force. In the following we assume that F is proportional to the length of the cilia bands as suggested by Hansen (Hansen, 1991) and we model the strength of the total cilia force as:

$$F = 2 \pi C_F \eta b U , \qquad (9)$$

where C_F is a dimensionless propulsion force coefficient that depends on geometry and distribution of the cilia and U is an effective time-averaged speed of the cilia motion. The propulsion force per unit cilia band length most likely increases as the larva grows and each cilium gets longer, but for simplicity we assume that $C_F\eta U$ is constant during the larval development. By balancing
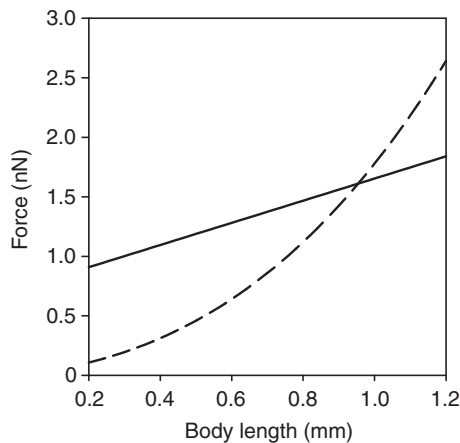
Fig. 5. Theoretical curves for propulsion force F (solid line) and buoyancy-corrected weight $m'g$ (dashed line) versus larval body length of *Polydora ciliata*. Note that the critical larval body length, l_{max}, corresponds to the point where the curves for F and $m'g$ intersect.
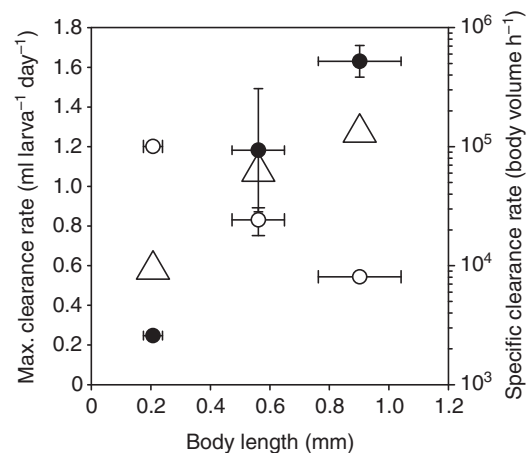

Fig. 6. Maximum clearance rate of *Polydora ciliata* larvae plotted *versus* larval body length. Black circles (left axis) show the maximum clearance rate (ml larva^{-1} day^{-1}); white circles (right axis) show the body volume specific clearance rate (body volume h^{-1}). Error bars indicate ±s.d. Open triangles show the model of the maximum clearance rate (Eqn 14).

the propulsion force F and the drag force D we obtain the swimming speed:

$$V = \frac{5\,C_F\,U}{3\,(4 + a/b)} \ . \tag{10}$$

The simple model (Eqn 10) predicts a slow decrease of the swimming speed in agreement with the observed horizontal swimming speeds (Fig. 4). Our fit of Eqn 10 to the measured horizontal swimming speeds determines the propulsion force per unit cilia band length to $C_F\eta U = 2.0\times10^{-6}$ N m^{-1}, where we have used $\eta = 1.00\times10^{-3}$ Pa s and a/b from our fit to the morphometrics of live larvae (Fig. 2).

Influence of gravity on swimming behavior

The larvae are slightly negatively buoyant, and the upward swimming speed V_{up} is therefore smaller than the downward swimming speed V_{down} (Table 1 and Fig. 4). In addition to the propulsion force F and the drag force D, the larvae are influenced by gravity, i.e. the buoyancy-corrected weight $m'g$, where m' is the buoyancy-corrected mass of the larva and g denotes the acceleration due to gravity. If we again model the larva body as a prolate spheroid we have:

$$m' = \frac{4}{3}\,\pi\,(\rho_s - \rho)\,a\,b^2 \ , \tag{11}$$

where ρ_s is the average density of the larva. The larva will evidently sink to the bottom if $m'g$ is larger than F. The buoyancy-corrected weight grows cubically with size, and if the propulsion force grows linearly with size, there will be a critical maximum body length l_{max} for which F and $m'g$ have the same magnitude. When the larva exceeds the critical body length, gravity will ultimately force the animal towards the sea floor. Using Eqns 9 and 11 and the force balance $F = m'g$ we obtain the following expression:

$$l_{max} = \sqrt{\frac{6\,(l_{max}/d_{max})\,C_F\,\eta\,U}{(\rho_s - \rho)\,g}} \ . \tag{12}$$

Eqn 12 shows that the maximum larval body length l_{max} increases as the square root of the propulsion force per unit length of the cilia

band $C_F\eta U$ and decreases as one over the square root of the excess density $\rho_s - \rho$. To compare the model with observations we plotted F and $m'g$ *versus* larval body length (l) using the excess density $\rho_s - \rho = 5$ kg m^{-3}, $g = 9.8$ m s^{-2}, l/d from our fit of the morphometrics of live larvae (Fig. 2), and $C_F\eta U = 2.0\times10^{-6}$ N m^{-1} from our fit of the horizontal swimming speeds (Fig. 4). The propulsion force is large compared with the buoyancy-corrected weight at small body length, whereas the reverse is true at large body length (Fig. 5). Using the above parameters we find the maximum larval body length $l_{max} = 0.95$ mm in good agreement with the observed body lengths for the largest free swimming larvae reported in nature. We return to the value of the excess density in the Discussion.

Maximum clearance and ingestion rates

The maximum clearance rate $\dot{Q}_{max}$ increased approximately proportionally to the larval body length, and the body volume specific clearance rate therefore showed a dramatic 10-fold decrease from 10^5 body volume h^{-1} in the early larval stage to
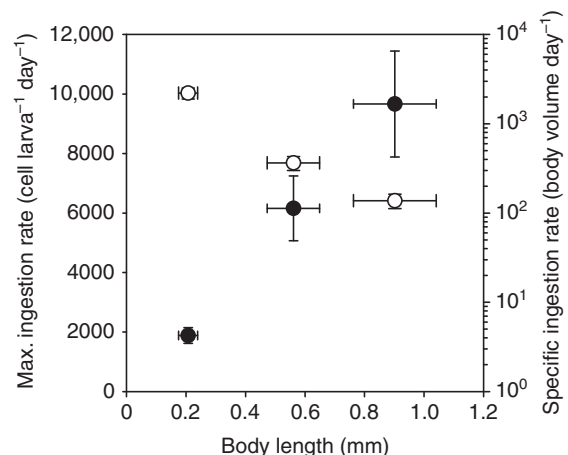

Fig. 7. Maximum ingestion rate of *Polydora ciliata* larvae plotted *versus* larval body length. Black circles (left axis) show the maximum ingestion rate (cell larva^{-1} day^{-1}); white circles (right axis) show the body volume specific ingestion rate (body volume day^{-1}). Error bars indicate ±s.d.
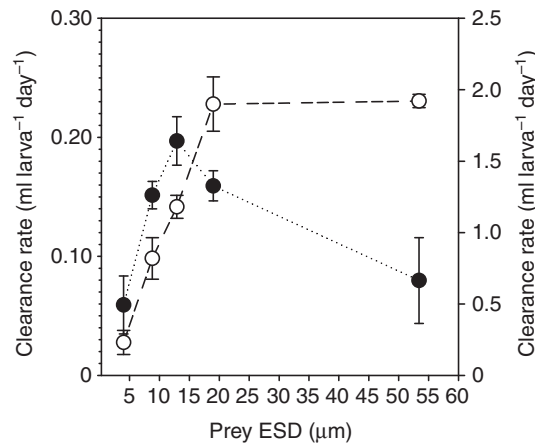
Fig. 8. Food size spectra for *Polydora ciliata* larvae. Clearance rate of early larvae (black circles; left axis) and late larvae (white circles; right axis) plotted *versus* the equivalent spherical diameter (ESD; µm) of the prey. Error bars indicate ±s.d.

Table 4. Clearance and ingestion rates obtained in *Polydora ciliata* larval incubation experiments in natural seawater (Isefjorden)

Property	Dinoflagellates	Ciliates
Initial concentration (cells ml^{-1})	411±45	4.04±0.74
Initial biomass (µg C ml^{-1})	4745±132	29693±65
Avg. Biomass (ng C ml^{-1})	0.77±0.02	10.09±0.03
Clearance rates (ml larva^{-1} day^{-1})	1.06±0.13	2.65±0.268
Ingestion rates (cells larva^{-1} day^{-1})	277±19	3.5±0.1
Clearance rates (ml larva^{-1} day^{-1})*	1.17±0.12	3.08±0.37
Ingestion rates (µg C larva^{-1} day^{-1})	0.224±0.012	0.037±0.001
Carbon specific ingestion (% day^{-1})	13.0±0.7	2.15±0.05
Volume specific ingestion (% day^{-1})	5.4±0.3	0.045±0.004

Values are based on the most abundant prey groups found. Note that clearance values marked with an asterisk are based on the per capita change in cell numbers whereas unmarked clearance rates are calculated from changes in prey biomass.
Values are means±s.d.

10^4 body volume h^{-1} found in the late larval stage (Fig. 6). The same characteristics are exhibited by the maximum ingestion rate $\dot{I}_{max}$ that increased from approximately 2×10^3 *Thalassiosira weissflogii* cells per larva per day to approximately 10^4 *T. weissflogii* cells per larva per day. A dramatic decrease in the body volume specific ingestion rate, similar to the decrease in the body volume specific clearance rate was likewise observed (Fig. 7).

To better understand the observed trends of the maximum clearance rate $\dot{Q}_{max}$ we modeled it as the product of the clearance area and the flow speed relative to the larva averaged over the clearance area. To estimate $\dot{Q}_{max}$ we assume that the maximum clearance rate is equal to the product of the area of the prototroch cilia band and the swimming speed of the larva:

$$\dot{Q}_{max} = \pi\,\alpha\,(2\,b + l_c)\,l_c\,V, \qquad (13)$$

where we have used l_c to denote the prototroch cilia length and where the dimensionless number α is used to take into account that the prototroch does not encircle the larva completely. Using the model expression for the swimming speed in Eqn 10 we obtain the expression:

$$\dot{Q}_{max} = \frac{5\,\pi\,\alpha\,C_F\,(2\,b + l_c)\,l_c\,U}{3\,(4 + a/b)}. \qquad (14)$$

Our observations of the prototroch cilia length, l_c, for the various larval stages gave $l_c = 27$ µm for the early stage, $l_c = 45$ µm for the intermediate stage, and $l_c = 48$ µm for the late stage (Table 2). With these values for l_c in the three larval stages and $\alpha = 0.75$ as suggested from sketches by Wilson (Wilson, 1928), we find that the model of $\dot{Q}_{max}$ using Eqn 14 overestimates the measured maximum clearance rate for the early stage, agrees well with the measured maximum clearance rate for the intermediate stage, and underestimates the measured maximum clearance rate for the late stage (Fig. 6).

Particle size selection

The larvae of *P. ciliata* are able to feed on prey ranging in size from 4 µm to 53 µm (Fig. 8). Clearance rates varied with prey size and larval length. The early larval stage displayed a maximum retention (optimal prey size) for particles of 12.9 µm and showed a reduced retention for smaller and larger particles. The late larval stage

retention increased with particle size until a maximum somewhere between 19 µm and 53 µm was reached.

Grazing on natural prey

The protist plankton community was initially dominated by the dinoflagellate *Heterocapsa triquetra* with more than 400 cells ml^{-1}, and its abundance exceeded the abundance of ciliates of approximately 4 cells ml^{-1} with a factor of 100. The ciliate community consisted mainly of *Strombidium* spp. Diatoms were scarce with only 0.1 cells ml^{-1} and they consisted mainly of *Ditylum* cf. *brightwellii* and *Coscinodiscus* spp. Feeding rates on dinoflagellates and ciliates are shown in Table 4. The dominance of *H. triquetra* made dinoflagellates the most important source of food for *P. ciliata* in this situation. However, ciliates that made a much less abundant food source were in fact cleared at a rate that was 2.5-fold higher than the clearance rate on *H. triquetra*.

DISCUSSION
Swimming patterns and speeds

No systematic differences in the patterns of the swimming paths related to larval size or food particle regime were observed, and we found similar swimming paths even when the larvae were exposed to 0.2 µm filtered seawater. Earlier observations, which were interpreted as raptorial feeding behavior, are most likely reactions to physical obstruction by a large particle as shown for gastropod veligers and calanoid copepodites (Hansen et al., 1991). Moreover, at any given larval development stage, the larval swimming paths of individuals were very variable (Fig. 3). This is also described by Wilson (Wilson, 1928) where the larvae frequently swims slowly rotating on their longitudinal axes, sometimes in circles about one place, and sometimes they curl up and erect their body spines when disturbed. We have speculated that the adaptive significance of an apparently non-predictable swimming path besides the spine erection could be a means of predator avoidance, but this remains to be verified.

The horizontal swimming speed decreases slowly with body length, which indicates that the propulsion force due to the ciliary swimming apparatus increases slower with body length than the drag on the body. Wilson (Wilson, 1928) suggested that body spines contribute negligibly to the drag, and that the notochord moderately or not at all contributes to the swimming force. Hence, we modeled the propulsion force as generated by the prototroch and the telotroch

solely. The decrease of the measured average horizontal speed is well described by the simple swimming model (Eqn 10 and Fig. 4) which takes into account that the larvae become relatively more slender (Figs 1 and 2) during their ontogenetic development. However, we speculate that our fit $C_F\eta U=2.0\times10^{-6}\,\mathrm{N\,m^{-1}}$ may be an underestimate of the cilia force per unit length of the cilia band, and also that the cilia force per unit length is not constant but increases slowly throughout larval development as each cilium gets longer. There are two main reasons for the possible underestimate of the propulsion force. First, in the simple model we balance the propulsion force due to the cilia swimming apparatus by the drag on a passively sinking prolate spheroid. In general the flow around a freely swimming larva is different from the flow around a passively sinking larva, and we note that our modeling approach does not take this into account. Langlois et al. (Langlois et al., 2009) considered a simple model of a self-propelled flagellate consisting of a spherical body with a cylindrical flagellum, and showed that the drag on the body is larger for a self-propelled flagellate relative to the drag on a passively sinking sphere. We presume that our estimate of the propulsion force for the swimming larvae similarly underestimates the true propulsion force, since we do not take into account the increase of the flow speed near the larval body due to the beating cilia. Second, the drag on the larval body may be larger than the prediction obtained from the prolate spheroid expression in Eqn 3, since this expression is derived for an object with a smooth surface and ignores the rough surface and setae structures on the larval body. This could lead to an underestimate of the propulsion force. Presumably this effect is more pronounced in the late larval stage, since the larvae at this stage begin to develop large palps (Fig. 1). Both a detailed morphological description of the cilia band structures and close observations of the metachronal wave of the beating cilia in swimming larvae in combination with direct numerical simulations of the flow past the larva would be needed to fully address these issues.

Planktotrophic larvae display actively phototactic behavior after hatching and this is also described for *P. ciliata* (Wilson, 1928). This is an adaptation to swim towards the photic zone of the water column where phytoplankton availability is highest. Later when approaching competence for metamorphosis they become negatively phototactic, which is interpreted as an adaptation to seeking settlement on the sea floor (Thorson 1950; Thorson, 1964). The relationship between propulsion force and gravity suggests that the hydrodynamic constraints could play a direct role in the settlement process (Fig. 5). The buoyancy-corrected weight of the slightly negatively buoyant larva becomes more and more important in comparison with the propulsion force as the larval size increases, and gravity therefore puts a final constraint on how large the larva can be without sinking. Eqn 12 suggests that the maximum body length l_{max} increases with increasing propulsion force per unit length of the cilia band $C_F\eta U$ and decreases with increasing density difference $\rho_s-\rho$. In our estimate we used the value $C_F\eta U=2.0\times10^{-6}\,\mathrm{N\,m^{-1}}$ obtained from our fit of the swimming model prediction to the measured horizontal swimming speed. We assumed that the larvae on average are 0.5% denser than water and found good agreement with the observation that the largest free swimming larvae have a body length of approximately 1.0 mm, which is supported by the findings by Hansen (Hansen, 1999). The larvae in the present study had up to 13 setigers where they at maximum can obtain 18 setigers and still be pelagic (Thorson, 1946). However, the largest possible value of the average larval density would be larger if the actual value of the cilia force per unit length is larger than our present estimate as discussed above. It is very challenging

to measure the excess density, since the larvae contract upon fixation, and we have not been able to find values for the excess density of polychaete larvae in the literature.

Maximum clearance rates

The propulsion force generated by the cilia apparatus of the larva balances the drag on the body of the larva when the larva is swimming freely with constant velocity. The net force exerted on the water by the larva is therefore zero and the flow relative to the larva is well approximated by a velocity field with parallel streamlines and constant flow speed equal to the swimming speed (Visser, 2001). The flow generated by a freely swimming larva differs from the flow generated by a larva that is tethered either by gravity as discussed by Strickler (Strickler, 1982) and Emlet and Strathman (Emlet and Strathman, 1985) or by mucous threads as explored by Fenchel and Ockelmann (Fenchel and Ockelmann, 2002). However, in general, the effect of tethering on the maximum clearance rate depends on the prey capture mechanism and the interaction between prey and cilia as discussed by Emlet (Emlet, 1990). We have not found evidence that *P. ciliata* larvae have mucous threads or that gravity, despite the observed effect on the upward and downward swimming speeds of *P. ciliata* larvae, should have a qualitative influence on the flow structure and result in an increase of the maximum clearance rate in the late larval stage.

The maximum specific clearance and ingestion rates should be measured using prey with size as close as possible to the optimal prey size, especially when comparing different developmental stages of given larvae. Here it was recorded on *Thallassiosira weisflogii*, which were close to the optimal prey size for both early and late larvae (Fig. 8). It was recorded to be higher than reported for *Mediomastus fragile* and *Marenzelleria* cf. *viridis* (Hansen, 1993; Burckardt et al., 1997), but similar to other ciliated larvae (Jespersen and Olsen, 1982; Hansen and Ockelmann, 1991). We assume that the particle capture is by the prototroch and maybe more ciliary structures in combination as described by Strathmann (Strathmann, 1971) and Hart (Hart, 1996). The measured maximum clearance rates are described reasonably well by Eqn 14, using 27 µm as the prototroch cilia length (l_c) for the early larval stage, 45 µm for the intermediate larval stage, and 48 µm for the late larval stage (Table 2; Fig. 6). The maximum clearance rate $\dot{Q}_{max}$ increased approximately proportionally to the larval body length, and the body volume specific clearance rate therefore showed a dramatic 10-fold decrease. Increasing clearance and ingestion rates as well as increasing optimal prey size has been demonstrated for crustaceans, e.g. the shrimp *Sergestes similis* and the copepod *Acartia tonsa* (Omori, 1979; Berggreen et al., 1988). However, specific food uptake rates declined with body weight (Omori, 1979) and optimal prey size remained constant for a ciliated gastropod veliger (Hansen and Ockelmann, 1991). Moreover, a thorough compilation of 13 echinoderm larval species reveals a substantial variation in feeding capabilities among larvae of similar size and shows that some are better suspension feeders than the others. Hence, no clear pattern in size-related clearance rate was detected (Hart, 1996).

Particle size selection

The ontogenetic retention spectrum exhibits a constant sized minimum prey, an increased optimal prey size and also an increased maximum prey size with larval body size. This is most probably related to the morphological constraints and the ontogenetic changes in the ciliary apparatus (Hansen, 1991; Riisgaard et al., 2000). However, in contrast to the opposed band veliger the maximum prey size for late *P. ciliata* larvae seems to be larger, which is

supported by late stage larvae when capturing motile oligotrich ciliates in the natural prey regime. This could be due to the increasing length of the prototroch cilia, dimensions of the mouth structure, or a contribution from the tentacles. Oral diameter is, for instance, described as being the upper limit for the size of prey for single band echinoplutei larvae (e.g. Rassoulzadegan et al., 1984). Since the principle behind food particle capture is not thoroughly understood we suggest that there should be further investigation of the morphology and functional capability of *P. ciliata* larvae. However, no matter how prey capture takes place the resulting principal ontogenetic changes in particle retention add to a reduction in intraspecific food competition among the various larval stages as suggested for a calanoid copepod (Berggreen et al., 1988).

Grazing on natural prey

When larvae were exposed to a natural prey field, ciliates were cleared significantly more than dinoflagellates, even though the dinoflagellate concentration was two orders of magnitude higher than the ciliate concentration (Table 4). Since dinoflagellates swim slower than ciliates (Hansen et al., 1997) and diatoms are non-motile in the water column, the higher clearance rates observed on ciliates, may be the results of a swimming-velocity-driven increased encounter probability of ciliates over the alternative prey particles (Jakobsen, 2005).

The larva did not display any specialized behavior as a response to the ambient prey regime. Not only do larval morphology and behavior govern larval feeding, prey behavior such as swimming speed also influence the feeding efficiency of *P. ciliata*. The larvae ontogeny seems to favor high prey uptake rates in the early stage with a remarkable 10-fold decrease of the specific clearance rate from 10^5 to 10^4 body volumes h^{-1} during ontogeny (Fig. 6). The same phenomenon is reported for larvae of *Philine aperta* with a factor of five decrease in maximum clearance during ontogeny (Hansen and Ockelmann, 1991). Additionally, a decrease in maximum specific clearance rate with size of zooplankton within the 2–2000 μm body size range reveals a common scaling factor of –0.23 (Hansen et al., 1997).

LIST OF SYMBOLS AND ABBREVIATIONS

a	larva model, polar radius (mm)
b	larva model, equatorial radius (mm)
c	larva model, geometric parameter (mm)
C_D	drag coefficient (dimensionless)
C_F	propulsion force coefficient (dimensionless)
d	larva diameter (mm)
d_{max}	maximum larva diameter (mm)
D	drag (nN)
F	propulsion force (nN)
g	acceleration due to gravity (m s^{-2})
$\dot{I}_{max}$	maximum ingestion rate (cell larva^{-1} day^{-1})
l	larva length (mm)
l_c	prototrochal cilia length (mm)
l_{max}	maximum larva length (mm)
m'	buoyancy-corrected mass of larva (kg)
$\dot{Q}_{max}$	maximum clearance rate (ml larva^{-1} day^{-1})
U	effective speed of the beating cilia (m s^{-1})
V	swimming speed, horizontal (mm s^{-1})
V_{down}	swimming speed, downward (mm s^{-1})
V_{up}	swimming speed, upward (mm s^{-1})
α	prototroch, geometric parameter (dimensionless)
η	dynamic viscosity (Pa s)
ρ	density of water (kg m^{-3})
ρ_s	average density of larva (kg m^{-3})
τ_0	larva model, geometric parameter (dimensionless)

REFERENCES

Almeda, R., Pedersen, M. T., Jakobsen, H. H. and Hansen, B. W. (2009). Feeding and growth kinetics by the planktotrophic larvae of the spionid polychaete *Polydora ciliata* (Johnston). *J. Exp. Mar. Biol. Ecol.* **382**, 61-68.

Anger, K., Anger, V. and Hagmeir, E. (1986). Laboratory studies of larval growth of *Polydora ligni*, *Polydora ciliata*, and *Pygospio elegans* (Polychaeta, Spionidae). *Helgoländer Meeresunters.* **40**, 377-395.

Berg, H. C. (1993). *Random Walks in Biology* Expanded Edition. Princeton, New Jersey, USA: Princeton University Press.

Berggreen, U., Hansen, B. and Kiørboe, T. (1988). Food size spectra, ingestion and growth of the copepod *Acartia tonsa* during development: implications for determination of copepod production. *Mar. Biol.* **99**, 341-352.

Blake, J. A. (1969). Reproduction and larval development of *Polydora* from northern New England (Polychaeta: Spionidae). *Ophelia* **7**, 1-63.

Bochert, R. and Bick, A. (1996). Reproduction and larval development of *Marenzelleria viridis* (Verril, 1973) (Polychaeta: Spionidae). *Mar. Biol.* **123**, 763-773.

Burckhardt, R., Schumann, R. and Bochert, R. (1997). Feeding biology of the pelagic larvae of *Marenzelleria* cf. *viridis* (Polychaeta: Spionidae) from the Baltic Sea. *Aquat. Ecol.* **31**, 149-162.

Daro, H. M. and Polk, P. (1973). The autecology of *Polydora ciliata* along the Belgian coast. *Neth. J. Sea. Res.* **6**, 130-140.

Dutz, J., Koski, M. and Jonasdottir, S. H. (2008). Copepod reproduction is unaffected by diatom aldehydes or lipid composition. *Limnol. Oceanogr.* **53**, 225-235.

Emlet, R. B. (1990). Flow fields around ciliated larvae: effects of natural and artificial tethers. *Mar. Ecol. Prog. Ser.* **63**, 211-225.

Emlet, R. B. and Strathman, R. R. (1985). Gravity, drag, and feeding currents of small zooplankton, *Science* **228**, 1016-1017.

Fenchel, T. (1988). Marine plankton food chains. *Ann. Rev. Ecol. Syst.* **19**, 19-38.

Fenchel, T. and Ockelmann, K. W. (2002). Larva on a string, *Ophelia* **56**, 171-178.

Frost, B. W. (1972). Effects of size and concentration of food particles on the feeding behaviour of the marine planktonic copepod *Calanus pacificus*. *Limnol. Oceanogr.* **17**, 805-815.

Hannertz, L. (1956). Larval development of the polychaete families Spionidae Sars, Disomidae Mesnil, and Poicilochaetidae n. fam. In the Gullmar Fjord (Sweden). *Zool. Bidrag. Uppsala* **31**, 1-204.

Hansen, B. (1991). Feeding behaviour in larvae of the opisthobranch *Philine aperta*. II. Food size spectra and particle selectivity in relation to larval behaviour and morphology of the velar structures. *Mar. Biol.* **111**, 263-270.

Hansen, B. (1993). Aspects of feeding, growth and stage development by trochophora larvae of the boreal polychaete *Mediomastus fragile* (Rasmussen) (Capitellidae). *J. Exp. Mar. Biol. Ecol.* **166**, 273-288.

Hansen, B. W. (1999). Cohort growth of planktotrophic polychate larvae - are they food limited? *Mar. Ecol. Prog. Ser.* **178**, 109-119.

Hansen, B. and Ockelmann, K. W. (1991). Feeding behaviour in larvae of the opisthobranch *Philine aperta* (L.) I. Growth and functional response at different developmental stages. *Mar. Biol.* **111**, 255-261.

Hansen, B. W., Hansen, P. J. and Nielsen, T. G. (1991). Effects of large nongrazable particles on clearance and swimming behaviour of zooplankton. *J. Exp. Mar. Biol. Ecol.* **152**, 257-269.

Hansen, P. J. (1989). The red tide dinoflagellate *Alexandrium tamarense*: Effects behaviour and growth of a tintinnid ciliate. *Mar. Ecol. Prog. Ser.* **53**, 105-116.

Hansen, P. J., Bjørnsen, P. K. and Hansen, B. W. (1997). Zooplankton grazing and growth: scaling within the 2-2000 μm body range. *Limnol. Oceanogr.* **42**, 687-704.

Happel, J. and Brenner, H. (1983). *Low Reynolds Number Hydrodynamics*, 2nd Edition. The Hague, The Netherlands: Martinus Nijhoff Publishers.

Hart, M. W. (1996). Variation in suspension feeding rates among larvae of some temperate, eastern Pacific echinoderms. *Invertebrate Biol.* **115**, 30-45.

Jakobsen, H. H., Halvorsen, E., Hansen, B. W. and Visser, A. W. (2005). Effects of prey motility and concentration on feeding in *Acartia tonsa* and *Temora longicornis*: the importance of feeding modes. *J. Plankton Res.* **27**, 775-785.

Jespersen, H. and Olsen, K. (1982). Bioenergetics in veliger larvae of *Mytilus edulis* L. *Ophelia* **21**, 101-113.

Langlois, V. J., Andersen, A., Bohr, T., Visser, A. W. and Kiørboe, T. (2009). Significance of swimming and feeding currents for nutrient uptake in osmotrophic and interception feeding flagellates. *Aquatic Microbial Ecol.* **54**, 35-44.

Menden-Deuer, S. and Lessard, E. J. (2000). Carbon to volume relationships for dinoflagellates, diatoms, and other protist plankton. *Limnol. Oceanogr.* **45**, 569-579.

NIMPIS (2002). *Polydora ciliata* species summary. National Introduced Marine Pest Information System (ed. Hewitt, C. L., Martin, R. B., Sliwa, C., McEnnulty, F. R., Murphy, N. E., Jones, T. and Cooper, S.). Web publication: http://crimp.marine.csiro.au/nimpis.

Omori, M. (1979). Growth, feeding, and mortality of larval and early postlarval stages of the oceanic shrimp *Sergestes similis* Hansen. *Limnol. Oceanogr.* **24**, 273-288.

Pedersen, T. M., Josefson, A., Hansen, B. W. and Hansen, J. S. (2008). Mortality through ontogeny of soft bottom marine invertebrates with planktonic larva. *J. Mar. Syst.* **73**, 185-207.

Pedersen, T. M., Almeda, R., Fotel, F. L., Jakobsen, H. H., Mariani, P. and Hansen, B. W. (2010). Larval growth in the dominant ploycheate *Polydora ciliata* is food-limited in an eutrophic Danish estuary (Isefjord). *Mar. Ecol. Prog. Ser.* **407**, 99-110.

Pernet, B. and McArthur, L. (2006). Feeding by larvae of two different developmental modes in *Streblospio benedicti* (Polychaeta: Spionidae). *Mar. Biol.* **149**, 803-811.

Plate, S. and Husemann, E. (1994). Identification guide to the planktonic polychaete larvae around the island Helgoland (German Bight). *Helgoländer Meeresunters.* **48**, 1-58.

Putt, M. and Stoecker, D. (1989). An experimentally determined carbon volume ratio for marine "oligotrichous" ciliates from eustraine and coastal waters. *Limnol. Oceanogr.* **34**, 1097-1103.

Rasmussen, E. (1973). Systematics and ecology of the Isefjord fauna. *Ophelia* **11**, 1-495.

Rassoulzadegan, F., Fenaux, L. and Strathmann, R. R. (1984). Effect of flavor and size on selection of food by suspension feeding plutei. *Limnol. Oceanogr.* **29**, 357-361.

Riisgaard, H. U., Nielsen, C. and Larsen, P. S. (2000). Downstream collecting in ciliary suspension feeders: the catch-up principle. *Mar. Ecol. Prog. Ser.* **207**, 33-51.

Schram, T. A. (1968). Studies on the meroplankton in the inner Oslofjord I. Composition of the plankton at Nakkeholmen during a whole year. *Ophelia* **5**, 221-243.

Strathmann, R. R. (1971). The feeding behavior of planktotrophic echinoderm larvae: mechanisms, regulation, and rates of suspension feeding. *J. Exp. Mar. Biol. Ecol.* **6**, 109-160.

Strickler, J. R. (1982). Calanoid copepods, feeding currents, and the role of gravity, *Science* **218**, 158-160.

Thorson, G. (1946). Reproduction and larval development of Danish marine bottom invertebrates, with special reference to the planktonic larvae in the sound (Øresund). *Medd. Kom. Dan. Fisk. Hav.* **4**, 1-523.

Thorson, G. (1950). Reproductive and larval ecology of marine bottom invertebrates. *Biol. Rev. Camb. Philos. Soc.* **25**, 1-45.

Thorson, G. (1964). Light as an ecological factor in the dispersal and settlement of larvae of marine bottom invertebrates. *Ophelia* **1**, 167-208.

Visser, A. W. (2001). Hydromechanical signals in the plankton. *Mar. Ecol. Prog. Ser.* **222**, 1-24.

White, F. M. (2006). *Viscous Fluid Flow,* 3rd Edition. New York City, USA: McGraw-Hill.

Wilson, D. P. (1928). The larvae of *Polydora ciliata* Johnston and *Polydora hoplura* Claparède. *J. Mar. Biol. Ass. UK* **15**, 567-603.

Zajac, R. N. (1991). Population ecology of *Polydora ligni* (Polychaeta: Spionidae). Seasonal variation in population characteristics and reproductive activity. *Mar. Ecol. Prog. Ser.* **77**, 197-206.